Beyond: Undergraduate Research Journal

Volume 2 Article 3

May 2018

Design and Development of a Magnetically-Driven Ventricular Assist Device (MVAD): In Vitro Implementation in the Fontan Circulation

Jansyn Johnston
Embry-Riddle Aeronautical University, johnj145@my.erau.edu

Christopher Adams
adamsc17@my.erau.edu

Design and Development of a Magnetically-Driven Ventricular Assist Device (MVAD): In Vitro Implementation in the Fontan Circulation

Cover Page Footnote

ACKNOWLEDGMENTS Arka Das, Ph.D. Student of Department of Mechanical Engineering, ERAU Anthony M. Khoury, Masters Student of Department of Mechanical Engineering, ERAU Kristin Sverrisdottir, Research Assistant of Department of Mechanical Engineering, ERAU Dr. Eduardo Divo, Associate Chair of Department of Mechanical Engineering, ERAU Dr. Anthony Nunez, Thoracic & Cardiac Surgery, Osceola Regional Medical Center Dr. Foram Madiyar, Department of Physical Sciences, ERAU Dr. Alain Kassab, Department of Mechanical and Aerospace Engineering, UCF

UNDERGRADUATE RESEARCH JOURNAL
Beyond

Design and Development of a Magnetically-Driven Ventricular Assist Device (MVAD): In Vitro Implementation in the Fontan Circulation

Jansyn Johnston and Christopher Adams

Abstract

A rapidly testable novel Magnetically-Driven Ventricular Assist Device (MVAD) with no moving parts that can be used to provide assistance to the cardiovascular circulation while reducing caval pressure in patients who have undergone the Fontan procedure to palliate the Hypoplastic Left Heart Syndrome (HLHS) is proposed and studied in this paper. A benchtop Mock Flow Loop (MFL) of the cardiovascular circulation with a Fontan total cavopulmonary connection (TCPC) is configured to validate this hypothesis. The MFL is based on a Lumped-Parameter Model (LPM) comprised of upper and lower systemic circulation as well as left and right pulmonary circulation compartments. Needle valves are used to accurately replicate vascular resistance (R) while compliance chambers are used to mimic vascular compliance (C). The MFL centerpiece is the truncated aortic arch with an implanted MVAD. A ferro-fluid solution is mixed in water to simulate magnetically-charged blood. The pulsating flow is induced by drawing the ferro-fluid from a main reservoir with a Harvard Apparatus Medical pump while the MVAD provides assistive momentum to the TCPC. Flow and pressure sensor data at specific points in the MFL are acquired via a National Instruments multichannel data acquisition board and processed using LabView. Different prototypes of the MVAD are tested to validate the hypothesis.

1. Introduction

Around eight percent of all newborns with a Congenital Heart Defect (CHD) have a single functioning ventricle. This condition is known as the Hypoplastic Left Heart Syndrome (HLHS) where the malformation of the left ventricle renders it minimally or non-functional and therefore the right ventricle is overloaded as it pumps both oxygenated and deoxygenated blood to parallel pulmonary and systemic circulations. As a result, research has been conducted towards the reduction of the load from the single ventricle. This can be achieved by establishing a connection between the systemic and pulmonary circulation resulting in a single univentricular pump powering the entire circuit, [1].

1.1 Palliative Procedure

A surgery is performed in three sequential stages to mitigate the flow pattern of HLHS:

Stage 1: Norwood

Stage 2: Glenn/Hemi-Fontan

Stage 3: Fontan

The Fontan operation has served as the 3rd stage palliation for this anomaly for decades but the surgery entails multiple complications and survival rate is less than 50% by adulthood. In this procedure, the Inferior Vena Cava (IVC) is disconnected from the right atrium and connected directly to the pulmonary arteries for a Total Cavopulmonary Connection (TCPC), [1]. This results in total passive drainage of the caval blood flow to the pulmonary circulation and therefore relieving the single ventricle from pumping blood to the pulmonary circulation.

1.2 Post-Fontan Paradox

The Fontan procedure often leads to multiple complications and survival rate of patients is of less than 50% by adulthood. The circulatory pattern of the patient can fail, even in patients with relatively good ventricular function. Pharmacological therapies have variable success and the probability of successful outcome with heart transplantation is low, [2,3].

1.3 Hypothesis

A novel alternative is proposed by creating a Magnetically-driven Ventricular Assist Device (MVAD) with no moving parts that can be used to provide assistance to the cardiovascular circulation while reducing the caval pressure. A bench top Mock Flow Loop (MFL) of the cardiovascular circulation with a Fontan TCPC coupled with the MVAD is configured to validate this hypothesis.

2. Governing Equations

A ferro-hydrodynamic (FHD) model, based on the Navier-Stokes equation, to estimate the average ferro-flow velocity is developed. This model considers

effective viscosity, magnetic flux density and volumetric concentration of the ferrous particles in the fluid. In this section, the governing equations to model the coupled problem provided by the fluid and the magnetic domain are discussed.problem provided by the fluid and the magnetic domain are discussed.

2.1 Fluid Flow Equations

The velocity field u of the fluid domain is governed by the Navier-Stokes equations such that,

$$\rho(\frac{\partial u}{\partial t}+u.\nabla u)=-\nabla p+F+\mu(\nabla^2 u) \quad (1)$$

Where ***F*** is the Volumetric Body Force exerted on the fluid. In the case of this experiment, the MVAD produces this body force as a result of the magnetic field acting on the ferrous nanoparticles.

2.2 Magnetic Force Equations

The magnetic force can be calculated such that,

$$F=(m\cdot\nabla)B \quad (2)$$

Where **m** is the magnetic dipole moment and **B** is the magnetic flux density provided by the inductance of the electromagnetic coil. The magnetic flux density is directly proportional to magnetic intensity with permeability constant, μ, for a particular medium, where,

$$B=\mu H \quad (3)$$

In this case, the working domain for the electromagnet is air, which has a permeability constant of 1.00000037. The following Maxwell field equations are used to quantify the magnetization effect of the developed electromagnet prototype:

Equations (4) and (5) are known as magnetostatics

$$\nabla\cdot B=0 \quad (4)$$

$$\nabla xB=\mu J+\mu\varepsilon\frac{\partial E}{\partial t} \quad (5)$$

$$\nabla\cdot E=\rho/\varepsilon \quad (6)$$

$$\nabla\times B=-\frac{\partial B}{\partial t} \quad (7)$$

equations and equations (6) and (7) are known as electrostatics equations. By using the Helmoltz theorem, it is known that **B** is an irrotational vector which can be expressed as,

Where ϕ is known as the magnetic scalar potential.

$$B=-\mu\nabla\varphi \quad (8)$$

The material property of the developed electromagnet depends on the magnetic moment, **m**. The magnetic susceptibility of a material within a magnetic field determines the tendency of the material to form a magnetic dipole. The magnetic susceptibility of iron is 3x104. Hence, the magnetic flux density can be rewritten as,

The magnetization vector **M** which determines the net

$$B=\mu(1+X)H \quad (9)$$

magnetic dipole of the material can be calculated as,

Hence, the magnetization vector can be defined as,

$$J=\nabla\times M \quad (10)$$

Therefore, by using the above equations, one may

$$M=XH \quad (11)$$

obtain the magnetic flux density provided by the electromagnet as,

Where B_{rem} is the remnant flux density.

$$B=\mu H+B_{rem} \quad (12)$$

3. Experimental Setup

3.1 Benchtop Model

A benchtop Mock Flow Loop (MFL) is designed to resemble the cardiovascular system of the target population for the palliative procedure, using a Lumped-Parameter Model (LPM) of the Fontan circulation anatomy with four branches, or lumps. These lumps represent the upper and lower systemic circulations as well as the left and right pulmonary circulations. Each lump is comprised of an area-reducing needle valve and a flow accumulator to model vascular resistivity and vascular compliance respectively. The MFL is driven by a Harvard Apparatus pulsatile pump.

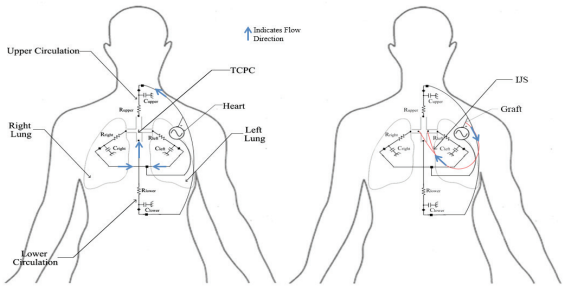

Figure 1: Lumped Parameter Model of the Body

It is important to note that the MFL is not an artificial equivalent of patient anatomy but rather represents an observable analogy of the anatomy, producing flow behavior that is physiologically relevant and accurate.

Since the MFL has many variables, a smaller closed loop consisting of a continuous pump and two flow meters was utilized during the calibrations and the testing of the MVAD prototypes. This closed loop assisted in obtaining accurate results with very few elements as compared to testing in the MFL.

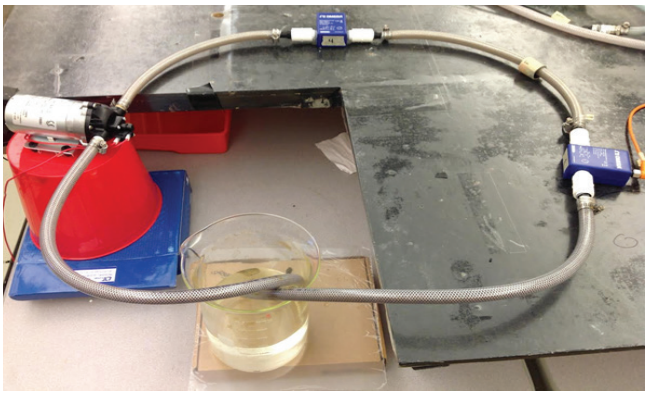

Figure 2 : Closed Loop Used for Calibrations and Testing

As shown, the two flow meters give the flow rate before and after the implementation of the MVAD prototype in order to monitor any change in flow.

3.2 Electromagnetic Flow Meters

The Electromagnetic Flow Meters that were purchased are the FMG90 Series by Omega and use no moving parts or obstructions. They measure the flow rate using magnetic induction to track the conductive particles of the passing fluid. Prior to implementing the flow meters into any testing, they were first calibrated using water. The flow meters were then calibrated using a Ferro-Fluid and water solution at three different concentrations in order to find any discrepancies in the frequencies measured while ferrous particles were introduced.

3.3 Dimensional Analysis

As the MFL will be operated using water instead of blood, it is important to match non-dimensional parameters to ensure physiologically relevant behavior. These non-dimensional parameters include the Womersley number, denoted α, and the Reynolds number, denoted Re. These non-dimensional parameters are matched by adjusting the Harvard Pump settings based on the MFL geometry. This process is described in Vukicevic's ,et.al., study on mock ciculatory systems [3].

3.4 Ferro-fluid

A Ferro-fluid is produced using an appropriate ratio of Ferrous Chloride ($FeCl_2^-$) and Ferric Chloride ($FeCl_3$) solutions mixed together in a base solution of ammonia (NH_3). The solution is kept at a steady temperature of around 50 degrees Celsius by resting on a hot plate under constant homogenization. Oleic Acid is used as a surfactant to inhibit clumping. The solution is centrifuged to eliminate ammonium hydroxide and to segregate the magnetite particles. The excess liquid is then replaced with Polyethylene Glycol (PEG). The diameter of the ferro-fluid particles is determined by placing a sample of the solution onto a silicon wafer for an examination in a Scanning Electron Microscope (SEM). The ferro-fluid sample is sputter coated with gold particles. For further investigation, the sample was put under a localized Energy-dispersive X-ray spectroscopy (EDX).

3.5 Magnetically-driven Ventricular Assist Device (MVAD)

According to equations (1) and (2), it can be seen that in order to maximize the acceleration of the fluid, one must maximize the magnetic flux density, or gauss (G) affecting the ferro-fluid. Additionally, it is imperative to minimize any obstruction of the flow due to the structure of the MVAD. To do so, the MVAD is essentially constructed by winding magnet wire around a hollow cylinder, which will be seated around the flow field, similar in fashion to an arterial stent. In the experimental development of the MVAD, several designs were considered with respect to core materials and winding configuration and then tested using a Gaussmeter. The Final MVAD Prototypes were tested in the closed loop using a 50% concentration of the ferro-fluid and water solution.

3.5.1 Preliminary Prototypes

The first manufactured prototypes were made using PTFE tubing with an inner diameter of 0.5 inches. PTFE insulated magnet wire of gauges 21, 28 and 35 were wrapped at an angle of 90 degrees with 80 wraps each, shown in Figure 3. Another prototype of the 35 gauge wire was wrapped at an angle of 75 degrees with 80 wraps as well. This was done in order to examine the change in magnetic flux when wrapped with different size wire and at different orientations.

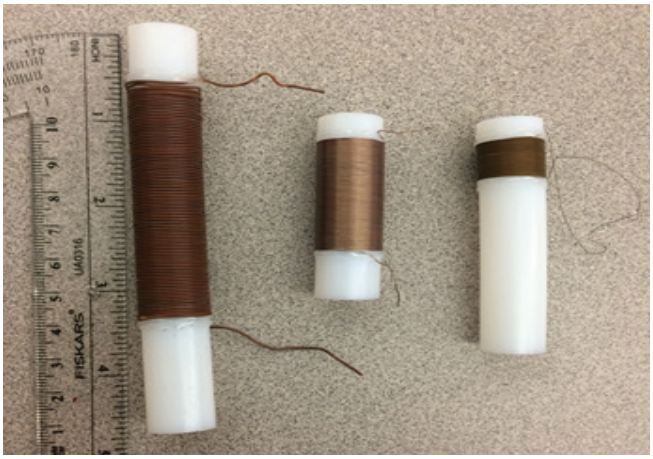

Figure 3 : Preliminary Prototypes made of PTFE Tubing and PTFE Insulated Magnet Wire

3.5.2 Black Iron Core Prototype

The Black Iron Core Prototype, shown in Figure 4, was tested in order to create a much larger amount of magnetic flux than the prior prototypes. From Equation 3, the permeability is directly proportional to the magnetic flux, therefore iron core was believed to create a stronger magnetic flux than the air core.

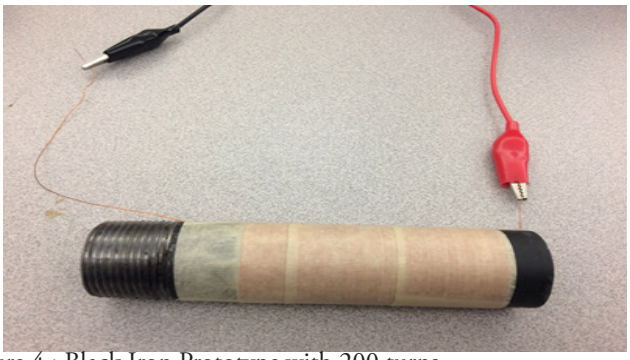

Figure 4 : Black Iron Prototype with 200 turns

3.5.3 Final Prototype A

This prototype was made of PVC piping with multiple layers of copper magnetic wire turns connected in parallel circuits. The multiple layers of turns increase the magnetic flux by increasing the number of turns while reducing the length of the electromagnet.

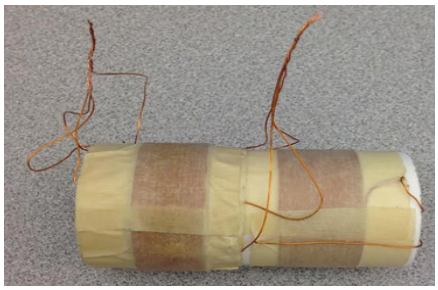

Figure 5 : Final Prototype A with 4 Layers of Copper Magnetic Wire

3.5.4 Final Prototype B

The next prototype was created in order to diminish the dipole effects as seen in Final Prototype A. These dipole effects were creating equal and opposite poles on the electromagnet, therefore thought to negate any potential increase in momentum. In order to reduce the dipole effect, six galvanized steel nails were inserted into the PVC pipe at an approximately 45 degree angle. The nails were then wrapped with 28 gauge wire and connected in parallel. The galvanized steel nails were selected because of the high magnetic permeability of the steel as a electromagnetic core.

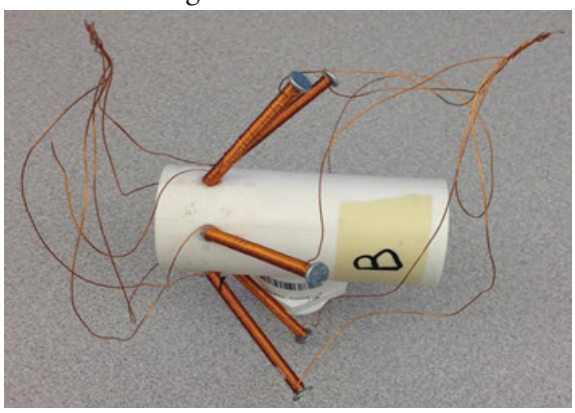

Figure 5 : Final Prototype A with 4 Layers of Copper Magnetic Wire

3.5.5 Final Prototype C

Similar to Final Prototype B, this prototype aimed to diminish the dipole effects seen in a conventional symmetrically wrapped electromagnet. In order to do this, the distance between the turns at the negative pole was increased to reduce the amount of magnetic flux at that end and prevent a cancellation effect. The initial distance between the turns was zero and was increased steadily from the positive pole to the negative pole of the electromagnet. The hollow core was 3D printed fused deposition modeling that was designed with helical grooves outlining the turn pattern of the wire.

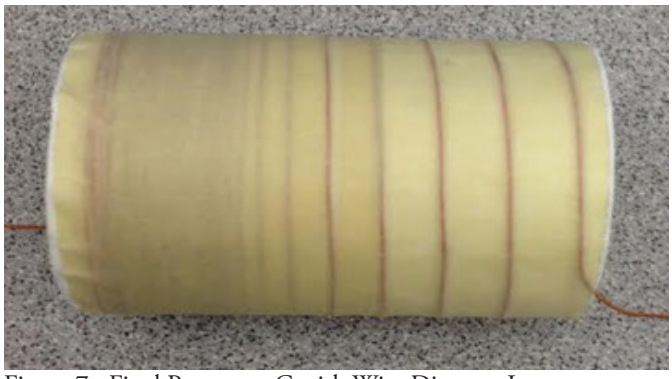

Figure 7 : Final Prototype C with Wire Distance Increase

3.5.6 Final Prototype D

The next prototype aimed to reduce the dipole effects using a helical pattern. The PVC pipe was wrapped with six magnet wire wrapped galvanized steel nails glued evenly around the pipe. They were spaced out along the length of the pipe so that the beginning of the next nail was at the halfway point of the previous creating an offset between the poles, shown in Figure 8.

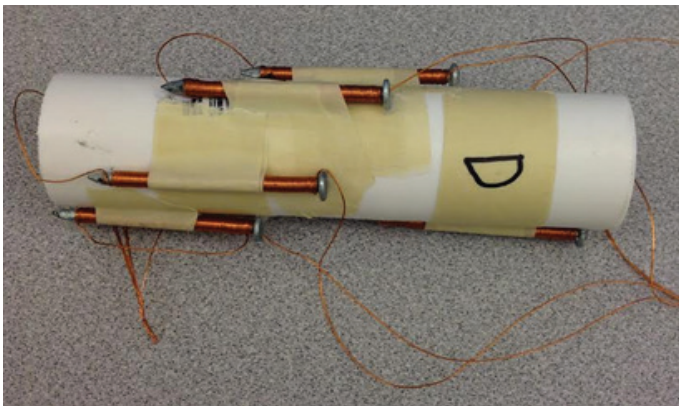

Figure 8 : Final Prototype D with 6 Galvanized Steel Nails Configured in a Spiral

3.5.7 Final Prototype E

The last prototype aimed to create a differentiation between the strength of the positive and the negative poles in order to reduce the dipole effect. The PVC was wrapped with four layers of magnet wire. The base layer was 75 turns and decreased by 15 turns outward, with each layer beginning at the start of the positive pole instead of aligning the centers of the layers. This focused the stronger effects created by the upper layers toward the start of the electromagnet.

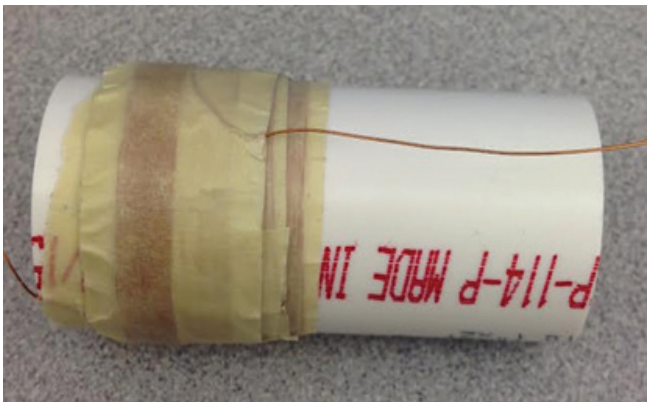

Figure 9 : Final Prototype E with Long to Short Layers of turns

4. Results

The results of the prescribed experimentation are summarized as follows.

4.1 Ferro-fluid

The average diameter of the particles is 147 nm (see Fig. 10).

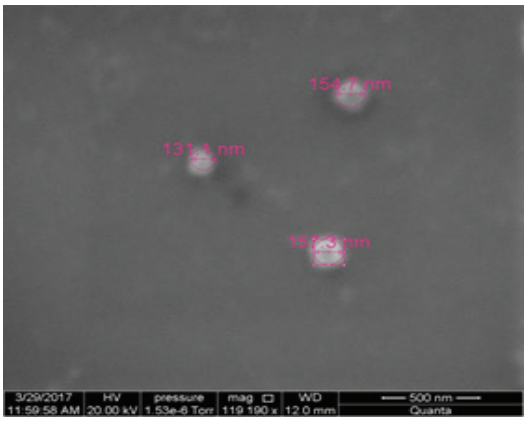

Figure 10: Nanoparticles under SEM with magnification factor of 119190

The SEM results confirmed that the ferro-fluid particles were small enough to create a homogenous solution when combined with water. Therefore, the MVAD would theoretically propel not only the ferrro-fluid particles, but the mixture of ferro-fluid particles and water.

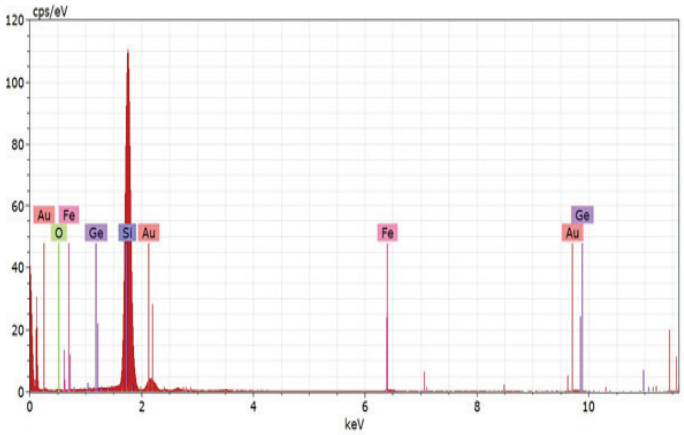

Figure 11: Distribution of elements present in EDX sample along with their energy levels

Element	Atomic Number	Normalized Weight (%)
Silicon	14	82.4
Gold	79	9.6
Oxygen	8	3.3
Germanium	32	2.8
Iron	26	2.0

Table 1: Elements present in EDX sample and respective normalized weights

It can be seen in Figure 11 that the sample contains iron (Fe) particles at two different energy levels, (K_α and L_α) along with germanium (Ge) and other chemicals in small amounts. The gold (Au) detected in the EDX sample is a result of the sputter coating of the particles. Also, the silicon (Si) results from the silicon wafer on which the specimen is placed.

4.2 Electromagnetic Flow Meters

The Electromagnetic Flow Meters were first calibrated using only water to find a baseline flowrate versus frequency equation. Each of the four flow meters displayed similar and accurate trends, shown in the example of flow meter 4 in Figure 12.

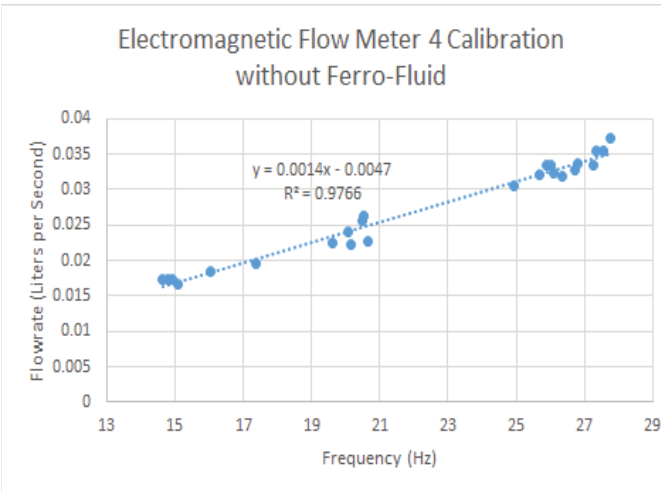

Figure 12: Calibration of Electromagnetic Flow Meter 4 with water

The flow meters were then tested at a constant flowrate, but with variation in concentration of Ferro-fluid and water solution. The low standard deviations of each of the different concentrations showed that the frequency would not fluctuate significantly between concentrations, shown in Table 2.

Electromagnetic Flow Meter Ferro-Fluid Calibration				
Ferro-Fluid Connentration	Average Frequency (Hz)			
	EFM 1	EFM 2	EFM 3	EFM 4
10%	16.85437	16.51029	16.75414	16.43771
25%	16.96138	16.53581	16.75023	16.50967
37%	17.0828	16.53943	16.82479	16.50741
SD	0.093319	0.012967	0.034263	0.033403

Table 2: Calibration of the Electromagnetic Flowmeters at various concentrations of Ferro-Fluid and water solutions

Since the flowmeters displayed little variance in frequency between different concentrations of Ferro-fluid, they were then calibrated to find the flowrate versus frequency equation using the 10% concentration. Each of the four flow meters again displayed similar and accurate trends, shown in the example of flow meter 4 in Figure 13.

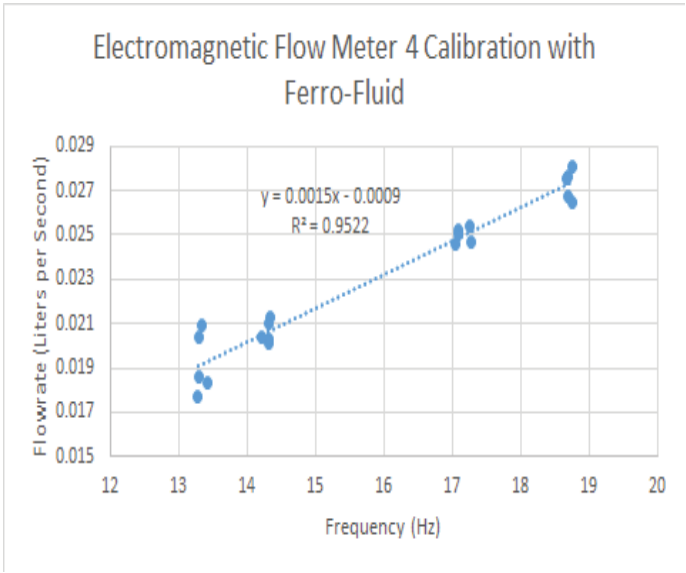

Figure 13: Calibration of Electromagnetic Flow Meter 4 with the 10% Ferro-Fluid and water concentration

4.3 Magnetically-driven Ventricular Assist Device (MVAD)

4.3.1 Preliminary Prototypes

The Preliminary Prototypes showed very minimal amounts of magnetic flux, only reaching values around 160 milligauss, shown in Figure 14. The prototypes showed little variance in magnetic flux with gauge, but provided insight into the fabrication with different sizes. The mid level 28 gauge wire proved to be the best option as it was less stiff than the 21 gauge, but conducted higher magnetic flux than the 35 gauge.

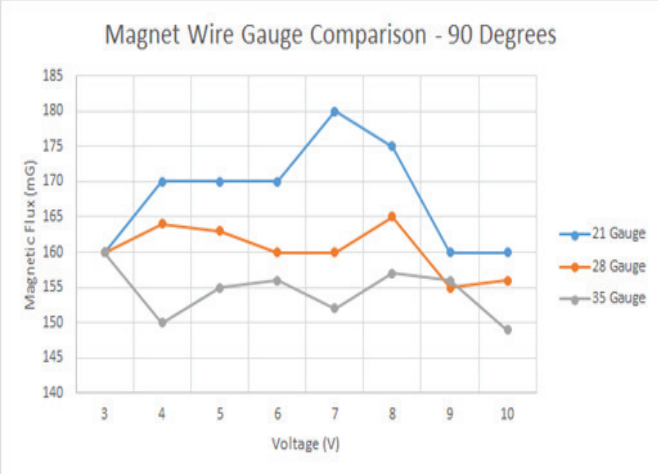

Figure 14 : Comparison of 21, 28 and 35 Gauge Magnet Wire Wrapped at 90 Degrees

The difference in angle with the 35 gauge wire showed that the wire wrapped at 90 degrees produced a higher magnetic flux than at 75 degrees, shown in Figure 16.

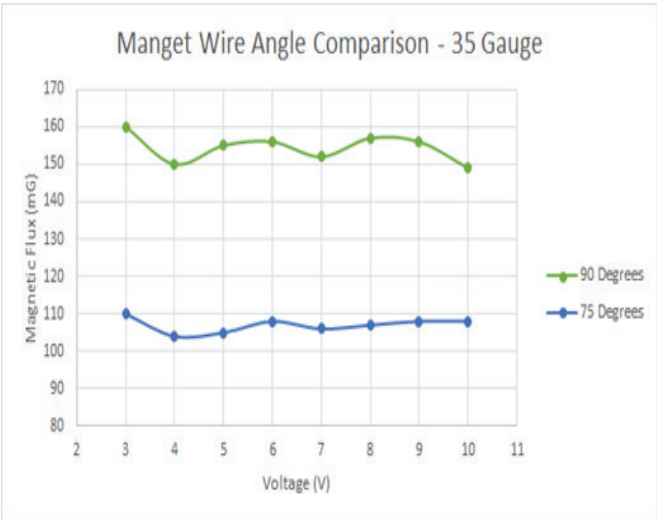

Figure 15: 35 Gauge Magnet Wire Wrapped to Compare Magnetic Flux at 90 Degrees and 75 Degrees

After testing the magnets with the Ferro-fluid in a thin plastic container, these small levels of magnetic flux could not cause any movement of the particles. The Ferro-fluid particles were then tested with a common bar magnet, which could move the particles with ease. The bar magnet produced levels of magnetic flux around 3 Gauss, which showed that the preliminary prototypes needed to provide much higher levels of magnetic flux.

4.3.2 Black Iron Core Prototype

Rather counter-intuitively, ferrous based cores proved ill-suited for this application. The ferrous core behaved as a sort of Faraday cage, absorbing the magnetic field generated by the inductive coil. This produced a large magnetic flux density within the bounds of ferrous material itself, but reduced the measureable Gauss present at the center of the annulus, the domain through which the fluid would flow. Due to this, a non-ferrous material is used in the construction of the Final MVAD Prototypes.

4.3.3 Final Prototypes

The Final MVAD Prototypes showed a decrease in the flowrate in both the flowmeter before the prototype and the flowmeter after the prototype as the amount of magnetic flux was increased, shown in Appendix I. The amounts of current applied to the prototypes vary due to the difference in wire resistivity. The testing was conducted with the continuous pump set at a flowrate of 1.618 Liters per minute. Final Prototype E showed the highest level of magnetic flux, yet still followed the trend of a decrease in flowrate.

Each of the prototypes showed the decrease in flowrate compared to the initial value, however Prototype B and C showed the largest decrease at their respective high level range of current, shown in Figure 16.

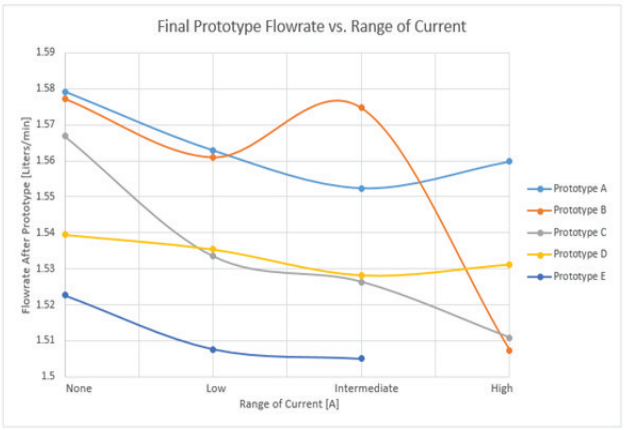

Figure 16: Final Prototype Output Flowrate at Various Currents

5. CONCLUSION

The results from the Final Prototype testing illustrate that the current prototype designs do not assist in the increase in flowrate of a Ferro-fluid solution. The preliminary prototypes were not creating enough magnetic flux while the black iron core was conducting enough magnetic flux, but the flux was solely concentrated on the pipe. As was seen in Appendix I, the highest magnetic flux from Prototype E, was not increasing the flow. Therefore, it can be concluded that

the strength of the magnetic field is not the limiting factor.

It is suspected that the polarization of the dipole effect is causing the decrease in flowrate. The higher magnetic flux density created at the center of the electromagnets is thought to be polarizing the ferrous particles prior to their exit of the device, momentarily suspending them. Hence, the initial flow is obstructed by the suspended ferrous particles which causes the observed decrease in flowrate. Due to the nano-size particles, the Ferro-fluid and water solution appears to remain homogeneous throughout the loop, but the ferrous particles may be experiencing a drag effect inside the prototypes due to the large flux density at the center. The Electromagnetic Flow Meters respond well to the addition of the Ferro-fluid to the solution, collecting accurate results within expected bounds.

6. Future Research

Based off the assumption that the ferrous particles are suspended in the center of the pipe at the highest magnetic flux density, a bypass will be added for the ferrous particles. The bypass will be inserted in the central location of the electromagnet with a tube intersecting the highest magnetic flux suspension. Some ferrous particles will escape through the bypass, therefore lessening the dipole effect of the negative pole of the electromagnet on the flow. The flow entering the bypass will then be reinserted to just before the prototype to be reintroduced to the flow. A basic prototype core without wire is shown for visualization in Figure 17.

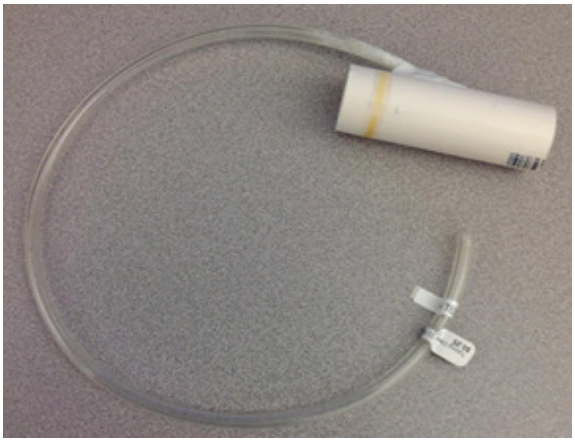

Figure 17: Basic Theoretical Prototype Design

References

[1] Fontan, F., and E. Baudet. “Surgical repair of tricuspid atresia.” Thorax 26.3 (1971): 240-248.

[2] Vukicevic M., Chiulli J.A., Conover T., Pennati G., Hsia T.Y., Figliola R.S. “Mock circulatory system of the Fontan circulation to study respiration effects on venous flow behavior.” ASAIO Journal (American Society for Artificial Internal Organs: 1992) 59.3 (2013): 253

[3] Das A., Khoury A., Tibbets J., Ni M., Divo E., Kassab A., DeCampli W. “Laboratory Development of a Self-Powered FONTAN for Treatment of Congenital Heart Disease.” Proceedings of the 2nd Thermal and Fluid Engineering Conference: (2017) and Aerospace Engineering, UCF

Appendeix I

Final Prototype Closed Loop Results					
Final Prototype	**Current [A]**	**Magnetic Flux [G]**	**Range of Current**	**Flowrate Before Prototpe [Liters/min]**	**Flowrate After Prototype [Liters/min]**
A	0	0	None	1.563307679	1.57923423
	2	27.9	Low	1.551200498	1.562852411
	4	55.4	Intermediate	1.539079687	1.552329872
	6	87.5	High	1.546328773	1.559747401
B	0	0	None	1.56496462	1.577248726
	3	8.8	Low	1.545818187	1.560953671
	6	16.7	Intermediate	1.561275085	1.574702167
	9	22.3	High	1.497361785	1.507320045
C	0	0	None	1.557746394	1.56689641
	1	12.4	Low	1.529464667	1.533471273
	2	21.6	Intermediate	1.519820328	1.526375421
	3	31.1	High	1.508925086	1.510826034
D	0	0	None	1.528782772	1.539445276
	3	9	Low	1.535974643	1.535392541
	6	14.9	Intermediate	1.520989655	1.528238513
	9	21	High	1.526039168	1.531232144
E	0	0	None	1.517641404	1.522587148
	1	61.4	Low	1.503708213	1.507637068
	2	118.8	Intermediate	1.502334809	1.504994627
	3	167.2	High	Heat Limiting	